

DOI: 10.1515/amm-2017-0180

W.J. KIM\*, H.-H. NGUYEN\*, H.Y. KIM\*, M.-T. NGUYEN\*, H.S. PARK\*\*, J.-C. KIM\*#

## SINTERING AND MICROSTRUCTURES OF SUS 316L POWDER PRODUCED BY 3D PRINTING PROCESS

Selective laser sintering (SLS) is a type of laminating sintering technique, using CO<sub>2</sub> laser with (metal, polymer, and ceramic) powders. In this result, the flake SUS 316L was used to achieve a high porous product, and compare to spherical type. After SLS, the porosity of flake-type sample with 34% was quite higher than that of the spherical-type one that had only 11%. The surface roughness of the flake SLS sample were also investigated in both inner and surface parts. The results show that the deviation of the roughness of the surface part is about 64.40 $\mu$ m, while that of the internal one was about 117.65 $\mu$ m, which presents the containing of high porosity in the uneven surfaces. With the process using spherical powder, the sample was quite dense, however, some initial particles still remained as a result of less energy received at the beneath of the processing layer.

*Keywords:* Stainless Steel, 3D-Printing, Selective laser sintering, SUS 316L, Flake powder

### 1. Introduction

Selective laser sintering (SLS) is one of the new rapid prototyping, tooling, and manufacturing technique with cost-efficient for a lot of applications such as automotive, aviation, mold, and machinery [1,2]. SLS has now been become an effective method for fabricating a number of various complex shapes, on not only metals but also polymers and even ceramics [3] compared to other sintering methods [4,5]. Additive manufacturing (AM) processes were initially proposed for producing prototypes, but in a few decades, their use changed and nowadays they are also employed for the fabrication of functional and structural parts for applying in industrial and medical fields. There are several processing methods belonging to the family of AM technologies. One of these processes is the selective laser sintering (SLS), which is based on local melting of a metal powder bed by a high power laser beam [6-9]. The SLS process provides many advantages compared to conventional methods, low surface quality is one of the major drawbacks encountered in the process. Secondly, in spite of the fact that the process is capable of making almost fully dense (~98-99%) parts, little residual porosity may still be problematic for some applications where high strength and fatigue resistance are necessary. In the scope of this study, laser re-melting is employed during or after the SLS process to overcome these problems [10]. In this process, powders are fused by high power laser beam into a product that has been desired with a three-dimensional shape by using modeling software such as computer-aided design (CAD) model or scan data [11,12]. Therefore, the powder is sintered layer by layer according to CAD model until the part build height is completed.

A number of grade powders have been used previously for manufacturing steel parts such as SUS 316 and 316L, 1080 steel by SLS process [13]. Usually in the SLS process, spherical powder has been used as a raw material to get the high surface roughness and high density. However, there are no results using non-spherical powders in the SLS technique to achieve the high porous product body.

The purpose of this paper is to present the results on the characteristics of the samples sintered by SLS printing process using flake and spherical types of the SUS 316L powders. Both power types were also compared in sinterability, porosity, and cross-section surface.

### 2. Experimental procedures

The SUS 316L powder with spherical and irregular shapes were used in this study. The composition of both types of SUS 316L powders is alike as displayed in Table 1 with the purity of 99.5% and supplied from Alfa Aesar. Particle size distribution of the powders was also investigated by particle size distribution (PSD) analysis. The powders were placed and sintered into the experimental apparatus of the SLS system (METALSYS 150) with the laser type of Yb fiber laser and laser wavelength of 1070 nm. The specimen was designed 10 $\times$ 10 $\times$ 10 mm<sup>3</sup>. The specimens were then analyzed by using field emission scanning electron microscope (FE-SEM – JEOL JSM 7500F) and optical microscopy (OM – Olympus PMG3). The Veeco Dektak 150 machine was carried out to examine the surface roughness of the SLS sample.

\* SCHOOL OF MATERIALS SCIENCE AND ENGINEERING, UNIVERSITY OF ULSAN, DAEHAK-RO 93, NAM-GU, ULSAN, 44610, REPUBLIC OF KOREA.

\*\* SCHOOL OF MECHANICAL ENGINEERING, UNIVERSITY OF ULSAN, DAEHAK-RO 93, NAM-GU, ULSAN, 44610, REPUBLIC OF KOREA.

# Corresponding author: jckimpml@ulsan.ac.kr

The composition of both SUS 316L powders

Element	C	Si	Mn	P	S	Ni	Cr	Mo
SUS 316L	0.03	1.00	2.00	0.04	0.03	12.00~15.00	16.00~18.00	2.00

### 3. Results and discussion

The characteristics of the SUS 316L powders with the difference in shape are shown in Figure 1. From Fig. 1(a) and (b) it can be seen that the non-spherical powder has the flake shape with the thickness of  $0.75\ \mu\text{m}$ , it could lead to the flowability of it during the SLS process under the effect of the laser beam. The average particle size measured by using particle size distribution (PSD) analysis was  $72.89\ \mu\text{m}$ . Fig. 1c and d show the morphology and particle size distribution of the spherical type powder. The average particle size was  $31.55\ \mu\text{m}$ . The differences about the size and shape of these powder somehow affects the sinterability of them and the quality of the final product.

Fig. 2 shows the polished surface of the network structure SLS sample molded with epoxy. The black area is the epoxy and the gray one is SUS 316L metal. By SLS, the powder was rearranged and networked together under high energy density laser beam. The powder was melted and interparticular necks were formed. During SLS processing, the temperature reached over the powder melting point, but not long enough for making a denser

structure before cooling down immediately. Therefore, the sample has high porosity of 34% with the density of  $5.33\text{g/cm}^3$ . After SLS, the initial flat and irregular powder was melted and its shape was transformed to round ones with the inter-particle connection. Furthermore, pores were also distributed quite homogeneously. I confirmed that it was possible laminated completely, but the fully dense sample is very difficult to be achieved.

The surface roughness of the non-spherical SLS sample investigated at the surface and internal parts are shown in Fig. 3. The red color represents the “+” deviation, and blue one indicates the “-” deviation. The average deviation of the roughness of the surface part is about  $64.40\ \mu\text{m}$ , while the roughness of the internal was about  $117.65\ \mu\text{m}$ . In fact, the laser touches to the surface of the upper parts was easier than to the uneven surfaces. It leads to the containing of the more porosity in the uneven surfaces. Moreover, in the internal structure, the distribution of not laminated portions and an uneven surface roughness was observed frequently.

Fig. 4 shows the polished cross-section surface of the SLS sample using spherical-type SUS 316L powder. The spherical

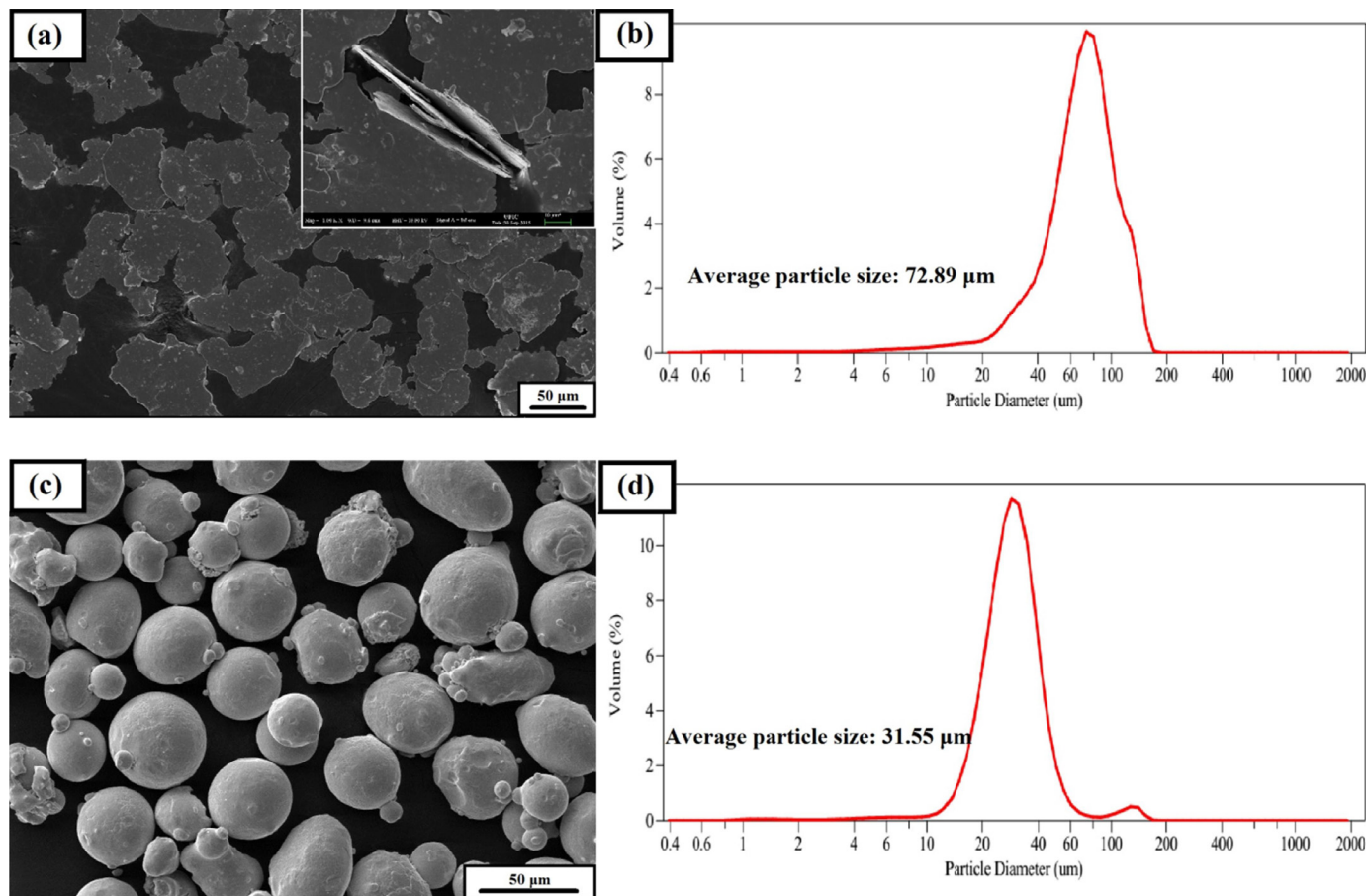


Fig. 1. The FE-SEM images and PSD analyses of (a) and (b) the as-received non-spherical, and (c) and (d) spherical powders, respectively

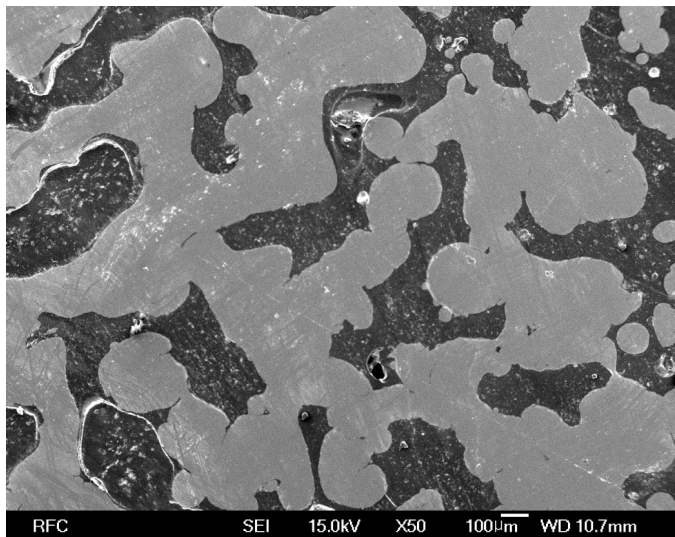


Fig. 2. The FE-SEM image of flake SLSed sample

shape have been commonly used to aid the flowability and reduce segregation, therefore, the sinterable and melting of particles were better than that of flat ones. The surface looks really dense with the distribution of small pores in the metal matrix. The density measured by Archimedes method was  $7.12 \text{ g/cm}^3$  with the porosity of 11%. The main reason for the difference between the samples using non-spherical and spherical powders is that the spherical powder has higher rearrangeability and smaller particle size. Therefore, the spherical powder was able to be sintered quicker with greater densification than the flake one.

Fig. 5 shows the fracture surface of spherical-type SLS sample. The initial spherical powder, which was mostly melted by high energy laser beam, could not be observed by FE-SEM. Moreover, this SLS process is pressureless, therefore, pores elimination carried out very slow. In addition, the melting time in the affected area is quite short leading to the existence of pores as seen in Fig. 5. There are some small initial powders

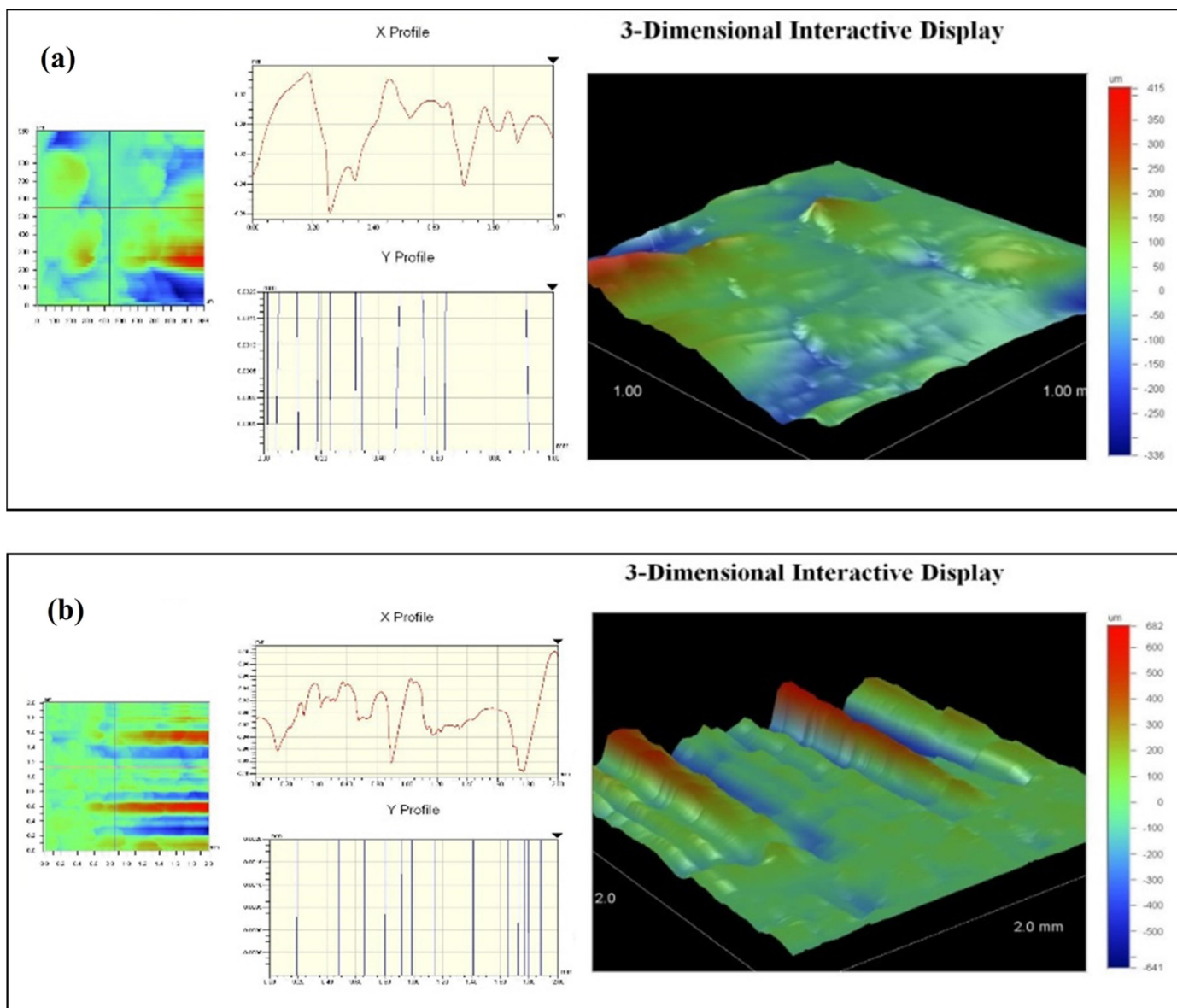


Fig. 3. The surface roughness of the flake-type SLSed SUS 316L sample at (a) the surface and (b) internal parts

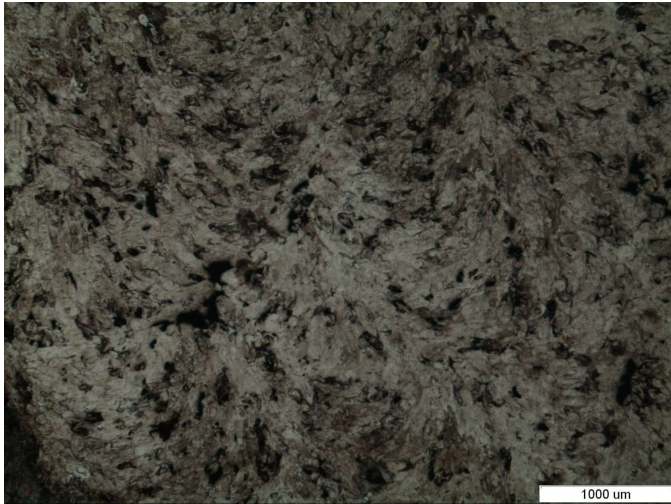


Fig. 4. OM image of spherical-type SLSed sample

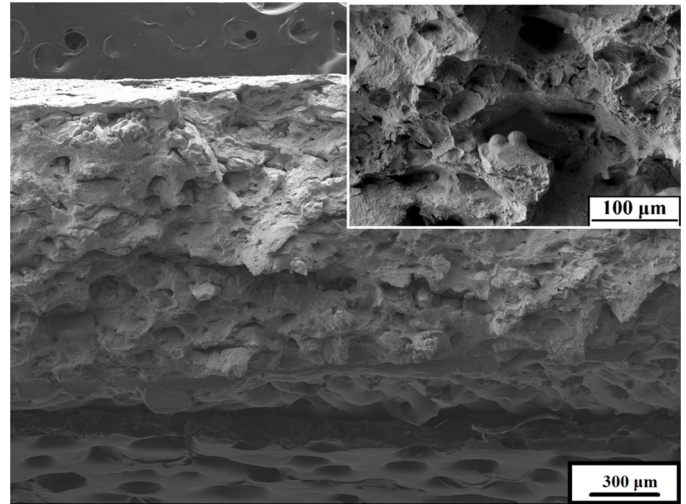


Fig. 5. Fracture surface of the spherical-type SLSed sample

remained. This phenomenon is explained by the laser affected area. After processing one layer, another layer will be added on to the previous one. The powders at the beneath of the processing layer will be received less energy than the above ones as a result of unmelted particles.

#### 4. Conclusion

The flake powder used sample has a porous structure with the porosity of 34%, while the spherical-type SLS one has only the porosity of 11%. After SLS processing, the initial flat and irregular powder was melted and its shape was transformed to round one with the interparticle connection. Many pores were observed in the non-spherical sample, which confirmed that the sample was laminated completely with a very porous metal body. For spherical powder, the initial shape was not observed after SLS, the sample was sintered well with dense in both cross-sectional and fractural surfaces. However, the tiny powders which were in the beneath of the processing layer were not melted and still in original shape.

#### Acknowledgements

This work was supported by the ICT R&D program of IITP/MSIP. (B0101-16-1081, Development of ICT based software platform and service technologies for medical 3D printing applications)

#### REFERENCES

- [1] C.R. Deckard, J.J. Beaman, P. 14<sup>th</sup> Conf. Prod. Res. Technol., Michigan 447-451 (1987).
- [2] J.P. Kruth, G. Levy, F. Klocke, T.H.C. Child, CIRP Ann. Manuf. Technol. **56**, 730-759 (2007).
- [3] E.O. Olakanmi, R.F. Cochrane, K.W. Dalgarno, Prog. Mater. Sci. **74**, 401-477 (2015).
- [4] H.H. Nguyen, M.T. Nguyen, W.J. Kim, H.Y. Kim, S.G. Park, J.C. Kim, J. Korean Powder Metall. Inst. **23** (3), 207-212 (2016).
- [5] Y.M. Kim, E.P. Kim, S.T. Chung, S. Lee, J.W. Noh, S.H. Lee, Y.S. Kwon, J. Korean Powder Metall. Inst. **20** (4), 264-268 (2013).
- [6] D.D. Gu, W. Meiners, K. Wissenbach, R. Poprawe, Int. Mater. Rev. **57** (3), 133-164 (2012).
- [7] Wohlers Report 2014, 3D Printing and Additive Manufacturing State of the Industry Annual Worldwide Progress Report, ISBN 978-0-9913332-0-2.
- [8] S.H. Huang, P. Liu, A. Mokasdar, L. Hou, Int. J. Adv. Manuf. Technol. **67**, 1191-1203 (2013).
- [9] W.E. Frazier, J. Mater. Eng. Perform. **23**, 1917-1928 (2014).
- [10] E. Yasa, J.-P. Krutha, Procedia Engineering **19**, 389-395 (2011).
- [11] E. Goode, Adv. Mater. Process. **161**, 66-67 (2003).
- [12] S. Kumar, JOM-J. Min. Met. Mat. S. **55** (10), 43-47 (2003).
- [13] J.P. Kruth, X. Wang, T. Laoui, L. Froyen, Assembly Autom. **23**, 357-371 (2003).